INFRARED EXTINCTION SPECTRA OF SOME COMMON LIQUID AEROSOLS

EDGEWOOD ARSENAL
ABERDEEN PROVING GROUND, MARYLAND

DECEMBER 1976

AD

EDGEWOOD ARSENAL TECHNICAL REPORT

ED-TR-77006

INFRARED EXTINCTION SPECTRA OF SOME COMMON LIQUID AEROSOLS

by

Hugh R. Carlon
David H. Anderson
Merrill E. Milham
Theodore L. Tarnove

Directorate of Development and Engineering

and

Robert H. Frickel
O. I. Sindoni, Ph.D.

Chemical Laboratory

December 1976

DEPARTMENT OF THE ARMY
Headquarters, Edgewood Arsenal
Aberdeen Proving Ground, Maryland 21010

Disclaimer

The findings in this report are not to be construed as an official Department of the Army position unless so designated by other authorized documents.

Disposition

Destroy this report when no longer needed. Do not return it to the originator.

REPORT DOCUMENTATION PAGE

READ INSTRUCTIONS BEFORE COMPLETING FORM

1. REPORT NUMBER: ED-TR-77006
2. GOVT ACCESSION NO.
3. RECIPIENT'S CATALOG NUMBER

4. TITLE (and Subtitle): INFRARED EXTINCTION SPECTRA OF SOME COMMON LIQUID AEROSOLS

5. TYPE OF REPORT & PERIOD COVERED: Technical Report, 1 January—30 November 1976

6. PERFORMING ORG. REPORT NUMBER

7. AUTHOR(s)
Hugh R. Carlon
David H. Anderson
Merrill E. Milham
Theodore L. Tarnove
Robert H. Frickel
O. I. Sindoni

8. CONTRACT OR GRANT NUMBER(s)

9. PERFORMING ORGANIZATION NAME AND ADDRESS
Commander, Edgewood Arsenal
Attn: SAREA-DE-M
Aberdeen Proving Ground, Maryland 21010

10. PROGRAM ELEMENT, PROJECT, TASK AREA & WORK UNIT NUMBERS
Task 1L662619AO6504

11. CONTROLLING OFFICE NAME AND ADDRESS
Commander, Edgewood Arsenal
Attn: SAREA-TS-R
Aberdeen Proving Ground, Maryland 21010

12. REPORT DATE: December 1976

13. NUMBER OF PAGES: 32

14. MONITORING AGENCY NAME & ADDRESS (if different from Controlling Office)

15. SECURITY CLASS. (of this report): UNCLASSIFIED

15a. DECLASSIFICATION/DOWNGRADING SCHEDULE: NA

16. DISTRIBUTION STATEMENT (of this Report)

Approved for public release; distribution unlimited.

17. DISTRIBUTION STATEMENT (of the abstract entered in Block 20, if different from Report)

18. SUPPLEMENTARY NOTES

Flame, incendiary, and smoke technology

19. KEY WORDS (Continue on reverse side if necessary and identify by block number)

Smoke	Scattering	Water fogs	Oil smokes
Optical extinction	Absorption	Sulphuric acid smokes	Atmospheric optics
Aerosol extinction	Spectral absorption	Phosphoric acid smokes	Liquid water content
Aerosol spectroscopy	Screening	Screening materials	Infrared

20. ABSTRACT (Continue on reverse side if necessary and identify by block number)

Infrared extinction spectra in the 3- to 5-μm and 7- to 13-μm atmospheric "window" regions have been obtained for smokes of petroleum oil, sulphuric acid, and phosphoric acid of varying droplet concentration, and for water fogs. Spectra were also obtained at 0.36 to 2.35 μm for petroleum oil and sulphuric acid smokes. Experimental results were compared, for sulphuric acid and water aerosols, to calculated values obtained from the Mie theory. Agreement was as good as ±10%. When absorbing smoke droplets are small compared to wavelength, very useful approximations apply and droplet clouds may be spectrally simulated by thin liquid films. In such cases, the imaginary component of refractive index may be approximated directly from aerosol spectra. At 12.5-μm wavelength, water fog extinction is nearly independent of droplet size distribution, suggesting a simple scheme for measurement of total liquid water content of an optical path.

PREFACE

This report summarizes the status of work performed under Task 1L662619AO6504, Flame, Incendiary, and Smoke Technology. The work was performed during the period of 1 January – 30 November 1976.

Its publication is intended to place in the hands of the user community extinction spectra of common military smokes and the means for interpreting these data and applying them to hardware requirements through recently developed techniques of aerosol spectroscopy.

Extinction data such as those reported here, combined with modeling to account for systems characteristics such as spectral response, contrast modulation and cloud travel, are fundamental to military screening and countermeasuring involving electro-optical systems operating in the visible and infrared wavelengths.

The use of trade names in this report does not constitute an official endorsement or approval of the use of such commercial hardware or software. This report may not be cited for purposes of advertisement.

Acknowledgment

The authors acknowledge with sincere appreciation the suggestions and comments offered by D. Deirmendjian (Rand Corporation, Santa Monica, CA), H. A. Gebbie (Appleton Laboratory, Slough, Barks., England), and G. Shaw (U. of Alaska, Fairbanks).

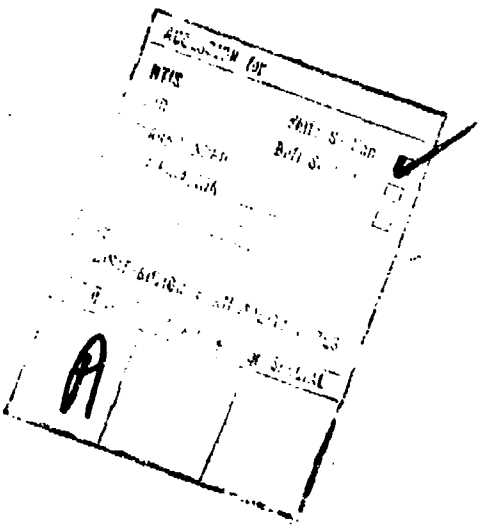

INFRARED EXTINCTION SPECTRA OF SOME COMMON LIQUID AEROSOLS

I. INTRODUCTION.

We have obtained infrared transmission data and extinction spectra for four common liquid-droplet smokes and fogs in the 3- to 5- and 7- to 13-μm atmospheric "window" regions. The materials investigated were petroleum oil smokes, smokes from burning phosphorus, sulphuric acid smokes, and artificial water fogs produced by condensing steam. In addition, spectra were run at 0.36 to 2.35 μm for petroleum oil smokes and sulphuric acid smokes. In ail cases, measurements were made also of liquid droplet concentration, droplet mass median diameter (MMD) and its geometric standard deviation, droplet chemical composition, relative humidity, and temperature. Where multiple scans were run, averages and standard deviations of experimentally determined extinction coefficients were computed.

Petroleum oil smokes, disseminated by thermal generation of military fog oil, are nearly classical scattering smokes. They have very little absorption (small imaginary index of refraction) in the infrared. Phosphoric and sulphuric acid smokes are strong absorbers in the infrared, particularly at longer wavelengths including the 7- to 13-μm region, where nearly all the observed extinction is due to the imaginary part of the complex refractive index.

Water fogs represent a spectrally hybrid class of aerosols which in typical droplet size distributions are good scatterers at shorter wavelengths and fairly strong absorbers at longer wavelengths. In the 7- to 13-μm region, for example, the contributions to total extinction of water fogs usually is divided about evenly between these mechanisms. When thermal equilibrium is attained between a water-containing cloud and its environment, the emissivity of the cloud approximates its absorptivity.

Phosphoric acid smokes were generated for our experiments by burning red phosphorus in air:

$$4P + 5O_2 = 2P_2O_5 \qquad (1\text{-a})$$

$$2P_2O_5 + 6H_2O = 4H_3PO_4 \qquad (1\text{-b})$$

$$4H_3PO_4 + 4n \cdot H_2O = 4H_3PO_4 \cdot nH_2O \qquad (1\text{-c})$$

Equations 1-a and 1-b represent chemical reactions with atmospheric constituents which proceed very rapidly, while equation 1-c represents equilibrium hydration of acid droplets by atmospheric humidity. Typical yields of acid smoke are three to four times the mass of phosphorus burned. Sulphuric acid smokes were produced by spraying a military smoke agent, FS, which is a solution of 55% SO_3 by weight dissolved in 45% by weight chlorosulfonic acid. When FS is sprayed into air containing even traces of moisture, it produces nearly pure sulphuric acid droplets plus a fraction of hydrochloric acid which quickly dissipates. Sulphuric acid smoke is extremely hygroscopic and attains a droplet acid concentration and thus a size distribution determined primarily by ambient relative humidity. Most sulphuric acid droplets generated in our trials contained between 30% and 45% by weight H_2SO_4.

II. INSTRUMENTATION.

Spectral measurements were made with instruments which were optically aligned through diametrically opposed 6-inch viewports in a vertical, 22-cubic-meter cylindrical thermally insulated steel test chamber having a height and diameter (optical path length) of 3 meters. Windows of 1.5 mil (0.0038 cm) polyethylene film were used where necessary with precautions to avoid condensation. Two chamber fans were run during observations to maintain homogeneous aerosol concentrations. The chamber could be rapidly exhausted. It had provision for water wash-down of the internal walls between trials and the means for introduction of steam if required. A spectrally scanning radiometer, described in an earlier paper[1] and modified to use liquid nitrogen cooling, was used to obtain spectra in the 3- to 5- and 7- to 13-μm infrared wavelength regions. This system was optically aligned upon a water-jacketed blackbody source in some trials and upon a blackened hotplate source in other trials where higher radiometric signal levels were desired. While extinction coefficients reported here were obtained primarily from "active" transmission spectra taken with a 400°C hotplate source, it was also possible to adjust the temperatures of the radiometer's internal reference blackbody and the water-jacketed cone on the opposite side of the chamber so that only emission signals from samples present in the chamber were recorded. Such "passive" measurements produced some very interesting results, particularly for condensing steam clouds, which will be the subject of a subsequent paper.

Also aligned across the chamber were a He:Ne laser (0.63 μm) with a power meter detector and a modified prism spectrophotometer with a chopped tungsten lamp source to scan the 0.36- to 2.35-μm wavelength region. Aerosol samples were drawn off periodically for analysis during the trials. Some of these samples were run through Anderson[2] cascade samplers which impacted particle fractions of known size ranges onto a series of eight preweighed, stainless steel plates. The total mass of aerosol deposited on each plate was determined gravimetrically and a chemical analysis for the mass of active component was also performed. An absolute filter following the plates trapped residual fine particles for analysis. A separate filter probe with calibrated airflow allowed total mass samples to be taken during trials for immediate weighing and determination of aerosol mass concentration. Through suitable calibration and procedures, it was possible to obtain good particle size and gravimetric data even for water fog droplets where evaporation of samples was an obvious complication. Commercial automatic (optical scattering) particle size measurement instrumentation was available but not applicable and was not used because of the high aerosol number concentrations needed for many of the measurements reported herein.

Humidity was determined by wet/dry bulb and gravimetric measurements. Thermocouple and thermistor networks were used for temperature measurements. Data were acquired directly on analog tape. Cross-computations with theoretical calculations (Mie theory) were performed for those smoke materials for which precise complex refractive index data were available. By such comparisons, the technology base and predictive modeling capabilities were expanded at the same time that experimental data were being collected for reference purposes.

III. PROCEDURE.

A smoke agent was generated and the resulting smoke was stirred by the chamber fans for several minutes to produce a homogeneous smoke concentration and size distribution. Spectral scans were run and data recorded while simultaneous measurements were made of particle size distribution and droplet mass concentration. Repeated measurements were made by venting the chamber stepwise to lower smoke concentrations. At the conclusion of a trial, the chamber was exhausted, washed down if necessary, and vented with ambient air.

Petroleum oil smokes were thermally generated using either a pyrotechnic generator which produced droplets in the 0.5-μm-diameter range or by dropping oil onto a hot surface which resulted in a larger droplet size distribution having an MMD of approximately 3.4 μm. Phosphoric acid smokes were generated by burning preweighed samples of red phosphorus (RP) in air. "FS" was spray-generated, and the resulting product was nearly pure sulphuric acid.

Water fog was generated by first introducing steam into the preheated chamber to achieve the desired droplet concentration, and then allowing slow cooling to sustain saturation humidity. In addition to the gravimetric and impactor techniques already mentioned, a method was developed to determine effective droplet diameter based upon simultaneous He:Ne laser transmittance readings at 0.63 μm and radiometer transmittances in the 8- to 13-μm wavelength region. This technique recently was reported in Applied Optics.[3] After an extensive search of infrared complex refractive index data in the literature, the values of Hale and Querry[4] (n - ik) were selected for all subsequent Mie calculations for water. These data have given consistently good agreement between theoretical and experimental results.

In some nonequilibrium conditions created in the chamber when fogs produced by condensing steam were allowed to cool, indications were seen of a bimodal distribution composed of smaller droplets having diameters in the 0.1- to 0.2-μm range and those of about 8- to 10-μm diameter. The smaller drops were presumed to be trying to grow on ambient condensation nuclei to larger diameters, but without sufficient water to do so. Initially, these constituted less than 10% of total mass liquid water (droplet) concentration, but in prolonged cooling trials their mass sometimes reached 70% or more of total droplet concentration as the 8- to 10-μm-diameter fraction dissipated. Their presence was deduced from simultaneous radiometer, laser, and gravimetric readings. Eventually, presumably at the point where saturation humidity could no longer be maintained in the chamber due to fog cooling, the 0.1- to 0.2-μm-diameter droplet fraction disappeared spontaneously and almost instantaneously. This could be observed most dramatically when the radiometer was operating in the "passive" mode with the water-jacketed cone blackbody as its source (target). In such cases, the radiometric (emission) signal from the cooling cloud dropped stepwise when the small droplet fraction disappeared, presumably by evaporation. Water remains one of the most difficult liquid aerosols to measure meaningfully and precisely. Its behavior and radiometric activity in transitions between the vapor and liquid states is only recently beginning to be understood.

IV. EXPERIMENTAL DATA.

The first data presented are those for military fog oil. Figures 1 through 3 show extinction coefficients for the visible and near infrared (0.36 to 2.35 μm), intermediate infrared (3 to 5 μm), and far infrared (7 to 13 μm) regions, respectively. These oil smokes were of the "normal" type, having MMD's of 0.58 μm ($\sigma_g = 1.45$) such as might be expected from a wide variety of oil smoke-producing sources found in the daily environment. An extinction coefficient of about 5.0 m^2/gm is found at 0.8-μm wavelength, representing a very large extinction value arising almost entirely from Mie-type scattering. The extinction coefficient falls rapidly with increasing wavelength until, in the 7- to 13-μm region of figure 3 (which averages two scans), almost no extinction is evident. Oil droplets, except for a few narrow bands shown by dashed lines in figure 2 near 3.5- and 4.3-μm wavelengths which are shared by the polyethylene chamber windows, have very little spectral absorption here. By using the hotplate method described earlier, larger droplet sizes were obtained for the oil smoke curves of figures 4 through 6 where the MMD was 3.4 μm ($\sigma_g = 1.7$). Because of the larger and broader droplet size distribution for these samples, a smaller peak extinction is found in the visible, but extinction by scattering is enhanced at longer wavelengths, especially in the 7- to 13-μm region.

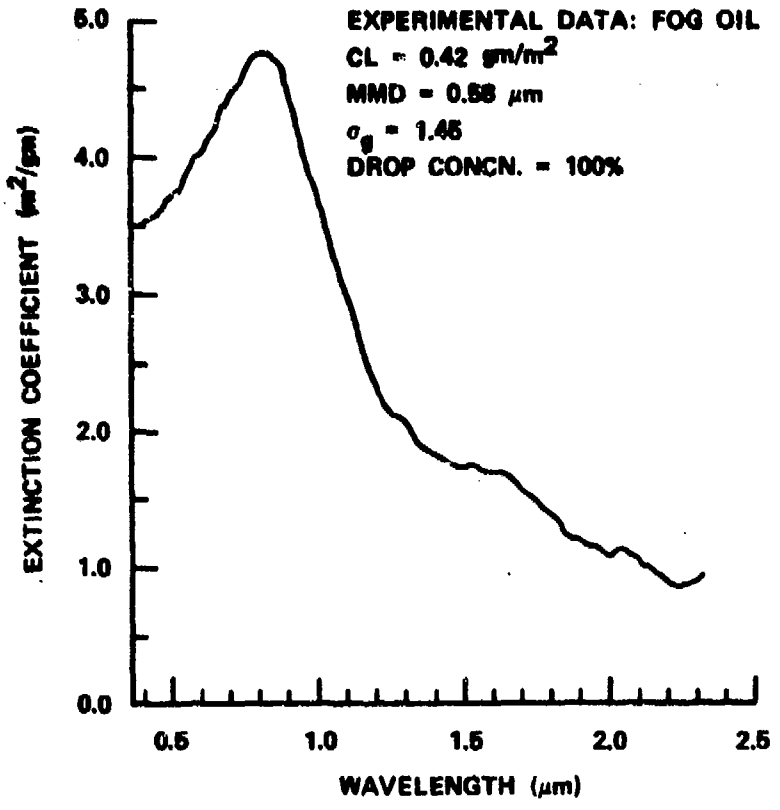

Figure 1. Experimental Data, Petroleum Oil Smoke, 0.58-μm MMD

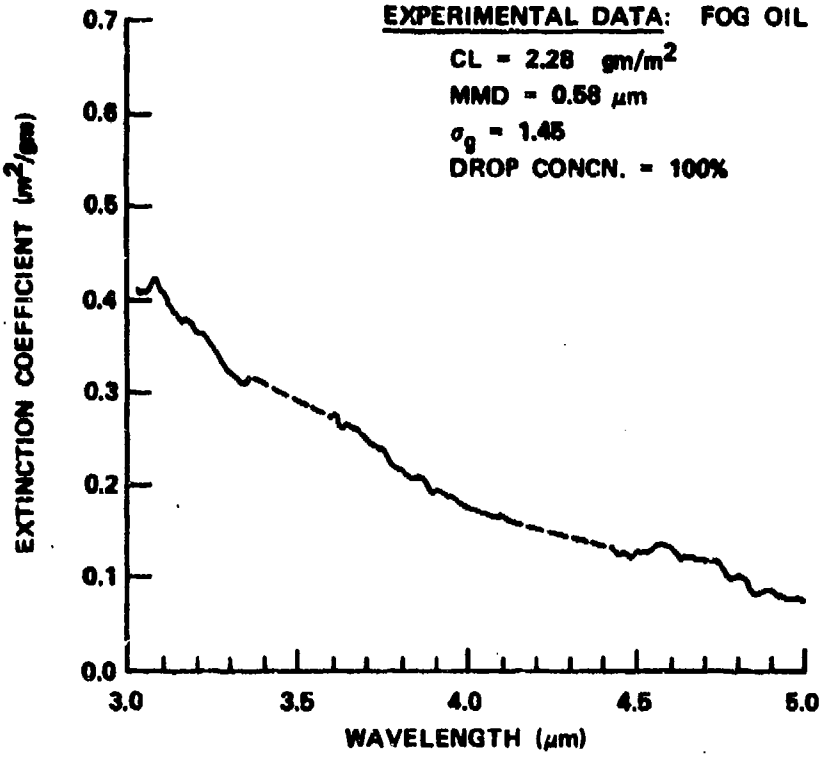

Figure 2. Experimental Data, Petroleum Oil Smoke, 0.58-μm MMD

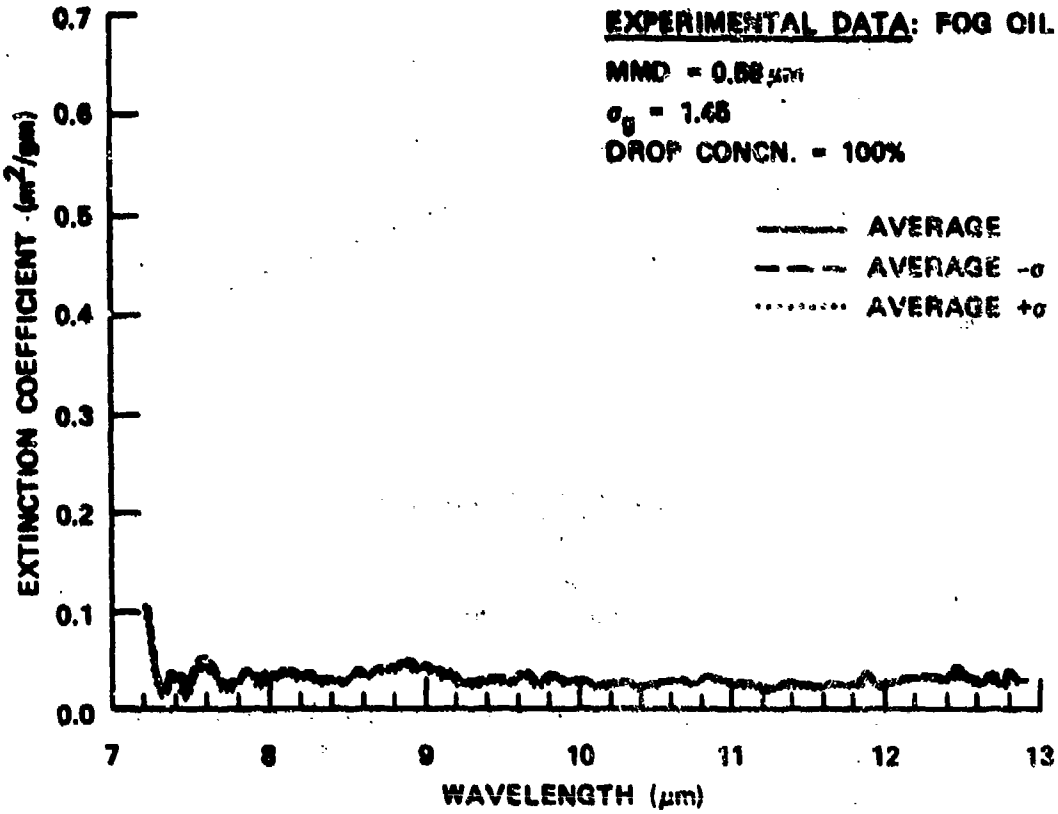

Figure 3. Experimental Data, Petroleum Oil Smoke, Average of Two Scans, 0.58-μm MMD

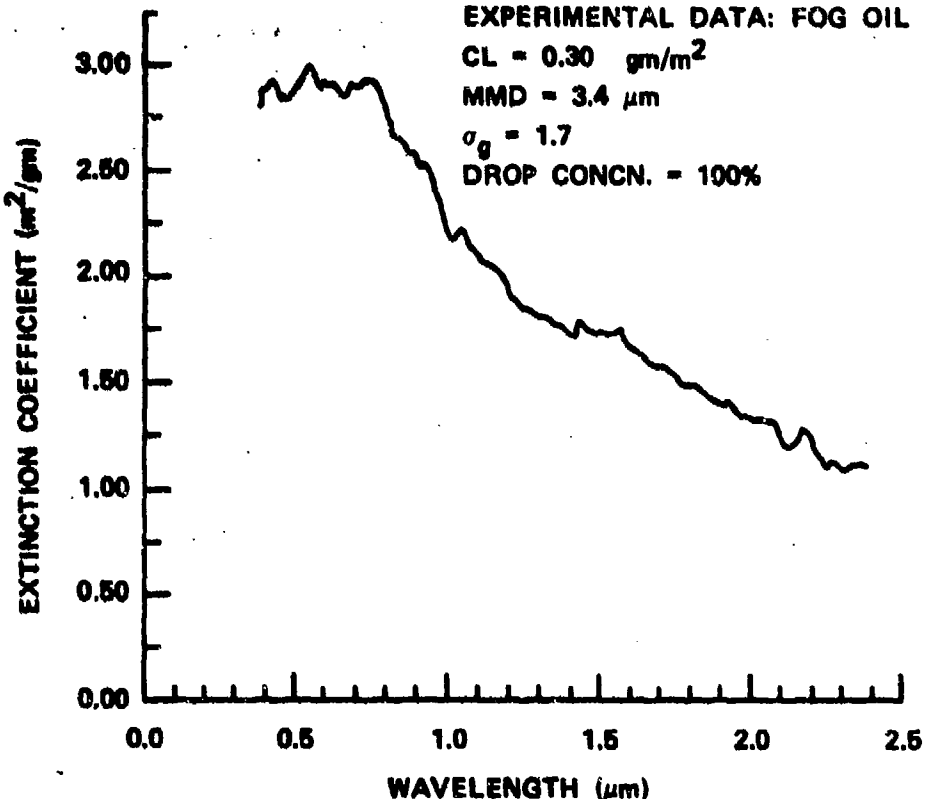

Figure 4. Experimental Data, Petroleum Oil Smoke, 3.4-μm MMD

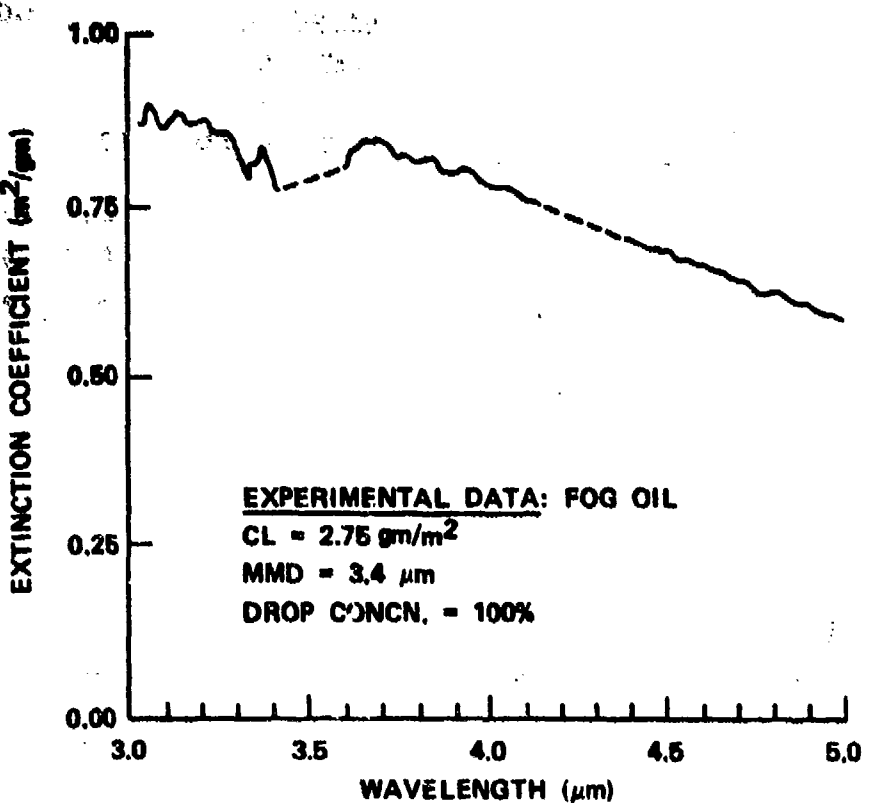

Figure 5. Experimental Data, Petroleum Oil Smoke, 3.4-μm MMD

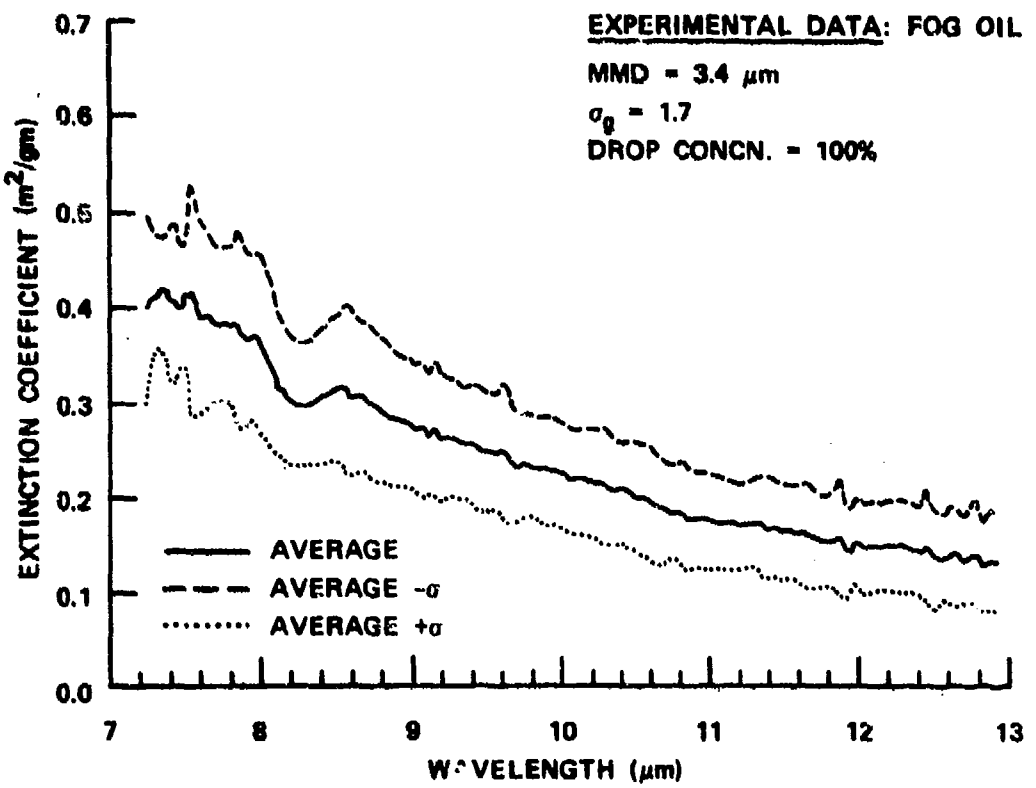

Figure 6. Experimental Data, Petroleum Oil Smoke, Average of Three Scans, 3.4-μm MMD

Compared to oil smoke, phosphoric acid smoke shows more infrared absorption, especially in the 7- to 13-μm region (figures 7 and 8). In figure 8, averages are shown for scans run at 5 CL values. The MMD's of 1.13 and 1.2 μm (σ_g = 1.4 and 1.7) are sufficiently small, as will be shown presently, to allow these smokes to behave almost as pure, Rayleigh-region absorbers in the far infrared. Therefore, the spectral features of figure 8 are very similar to those that would be observed in a liquid film absorption spectrum of the material comprising the droplets themselves—in this case, about 65% by weight phosphoric acid. The peaks near 8 and 10 μm are characteristic of phosphorus-oxygen compounds in this wavelength region, while the tail from 11.5 to 14 μm arises primarily from the water content of the droplets. The relative shapes of such curves, therefore, are very useful in deducing droplet acid concentrations or hydration levels.

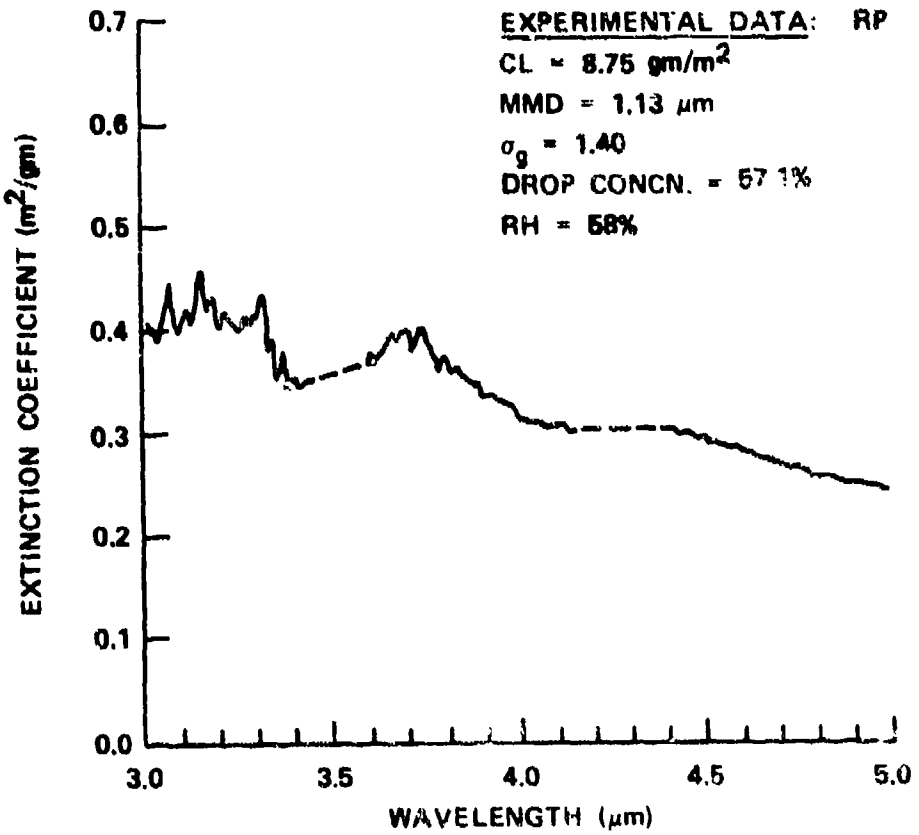

Figure 7. Experimental Data, Phosphorus (Phosphoric Acid) Smoke, 1.13-μm MMD

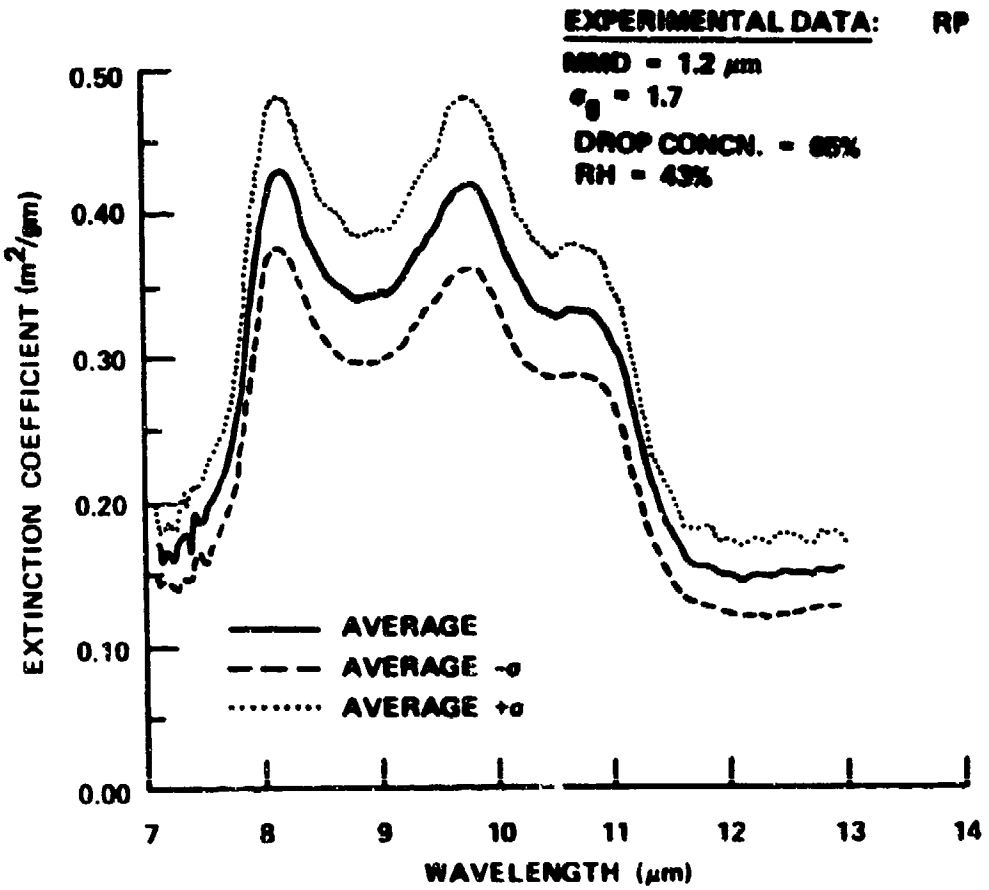

Figure 8. Experimental Data, Phosphorus (Phosphoric Acid) Smoke, Average of Five Scans, 1.2-μm MMD, Estimated

Figures 9 through 11 show the data obtained for two typical trials using agent "FS" to generate sulphuric acid smokes which in these trials contained 38% and 44% acid by weight in the average droplet. The MMD's of 0.78 and 0.85 μm (σ_g = 1.41 and 1.5) are smaller than those for phosphorus smokes, but their extinction coefficients are comparable as shown for data excerpts from figures 7 and 8. In figure 11, it can be observed that, because of the greater hydration of sulphuric acid smoke in this trial, the water tail from 10 to 14 μm is more pronounced than that shown in figure 8 for phosphoric acid smoke.

Figures 12 through 15 present data for water fogs formed by condensing and cooling steam down to 30°C.

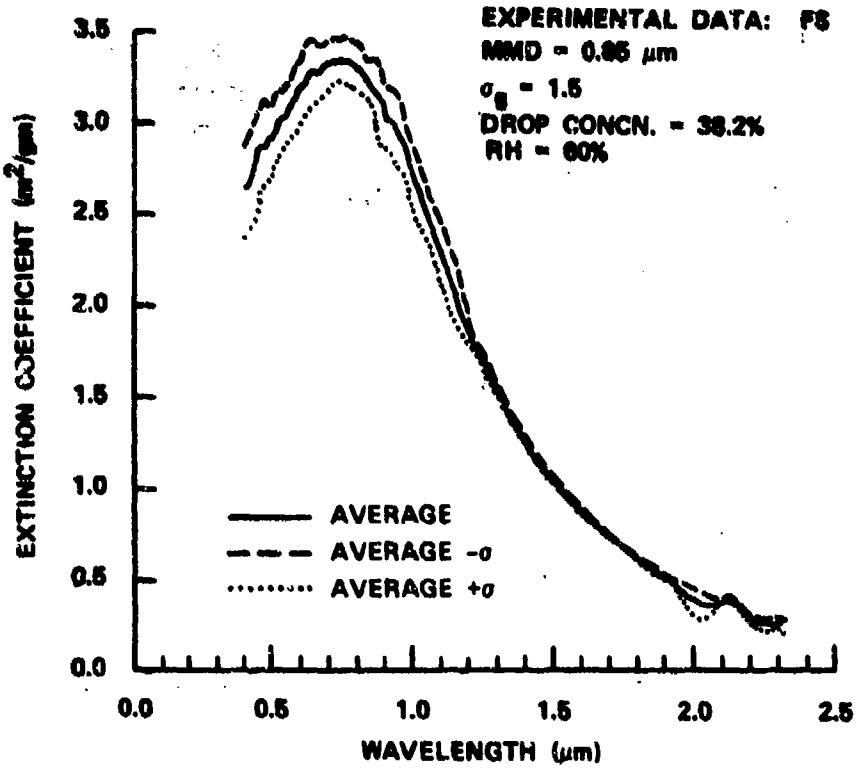

Figure 9. Experimental Data, Sulphuric Acid Smoke (FS), Average of Three Scans, 0.85-μm MMD, Estimated

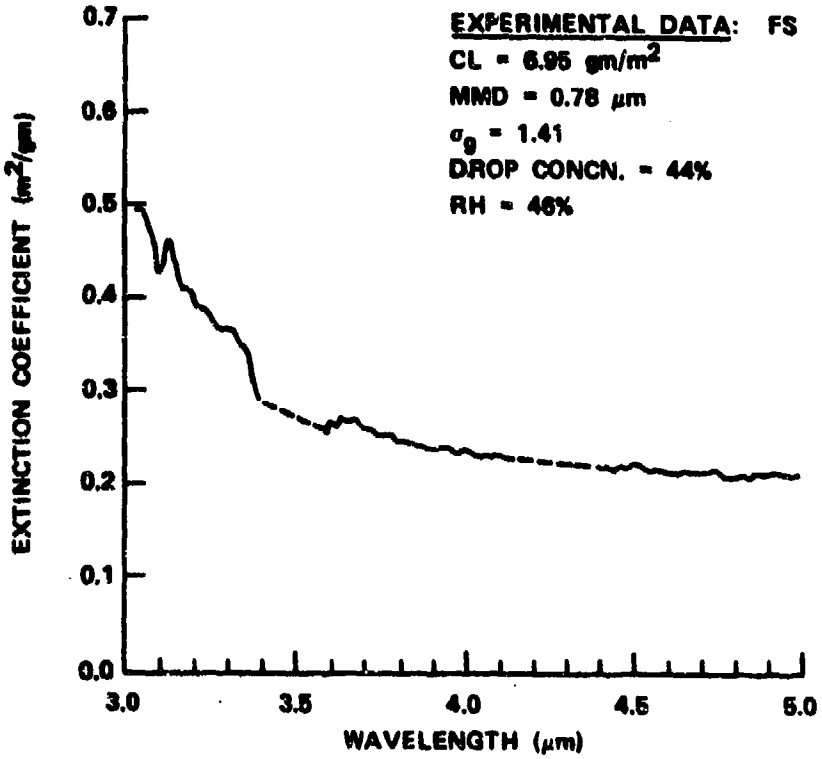

Figure 10. Experimental Data, Sulphuric Acid Smoke (FS), 0.78-μm MMD

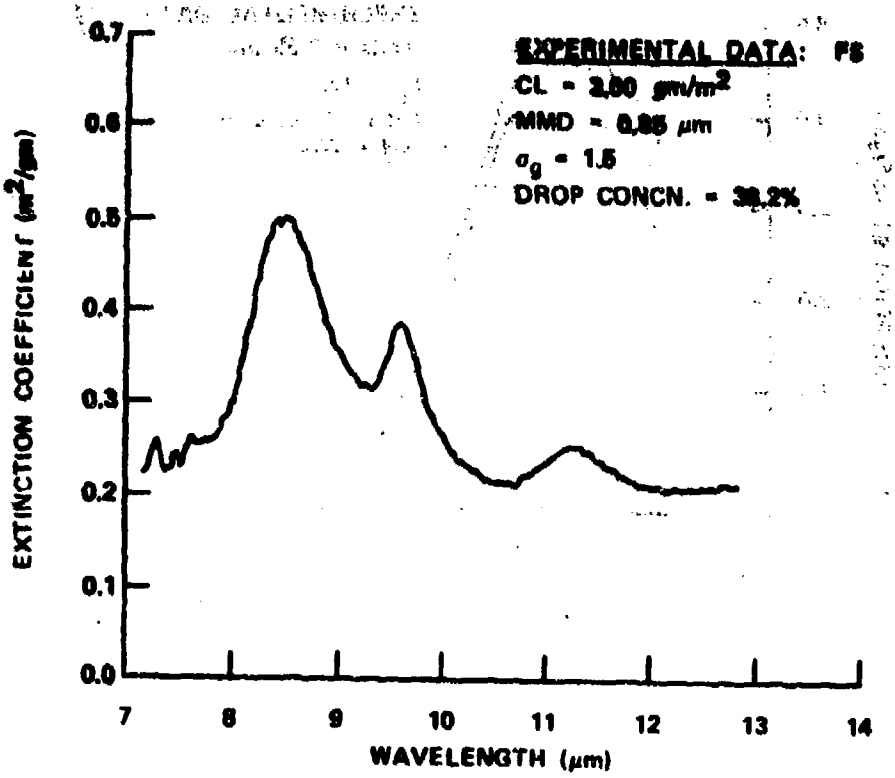

Figure 11. Experimental Data, Sulphuric Acid Smoke (FS), 0.85-μm MMD, Estimated RH = 60%

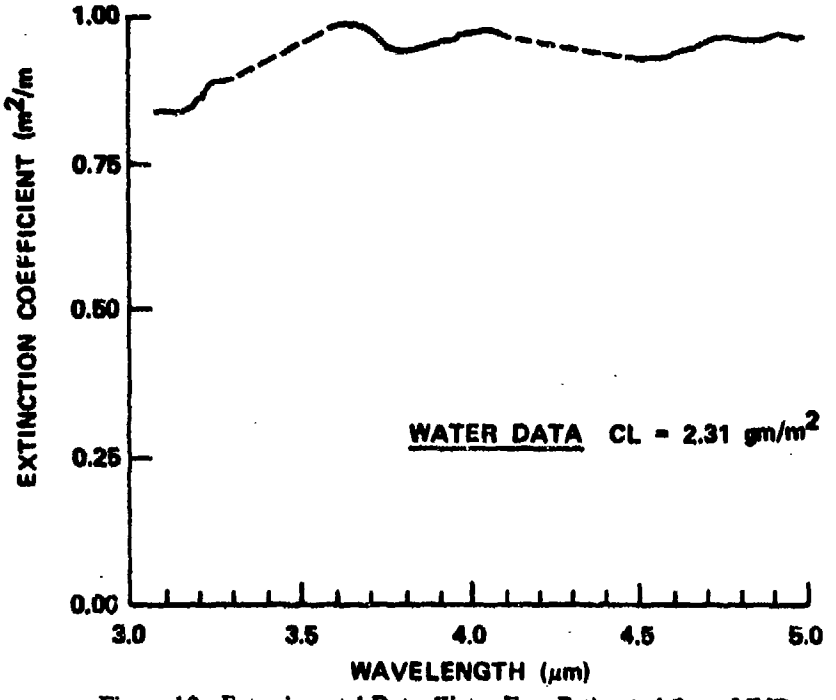

Figure 12. Experimental Data, Water Fog, Estimated 8-μm MMD, 100% RH, Drop Concn = 100% H_2O

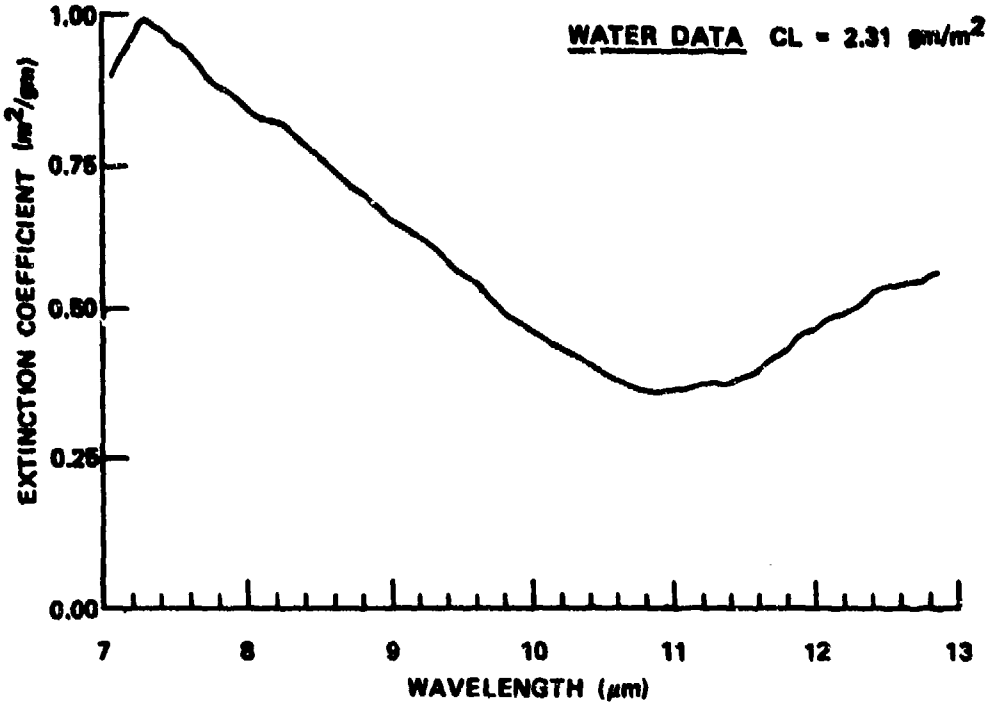

Figure 13. Experimental Data, Water Fog, Estimated 8-μm MMD, 100% RH, Drop Concn = 100% H_2O

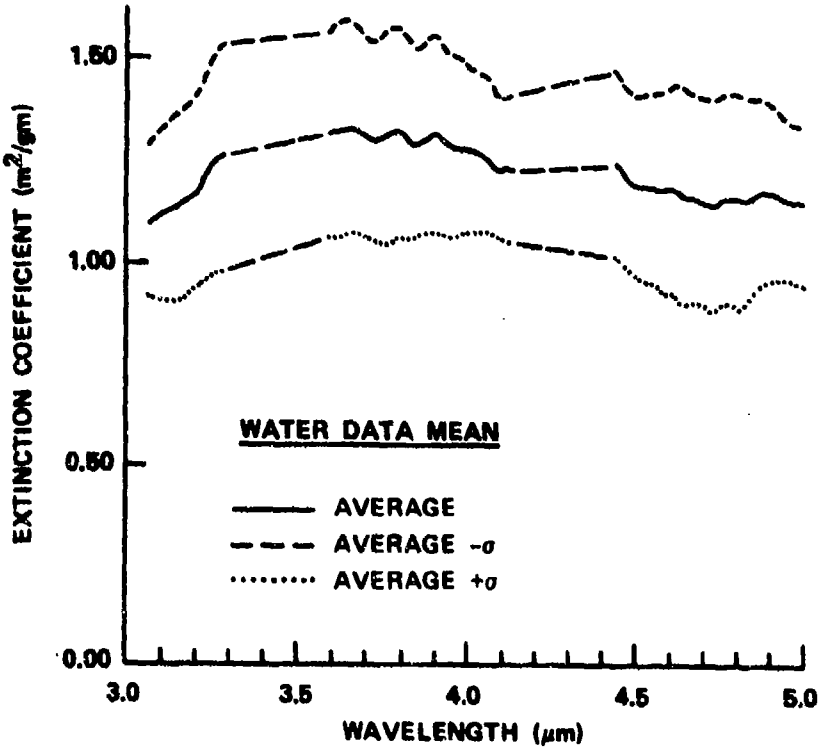

Figure 14. Experimental Data, Water Fog, Average of Five Scans, Estimated 8-μm MMD, 100% RH, Drop Concn = 100% H_2O

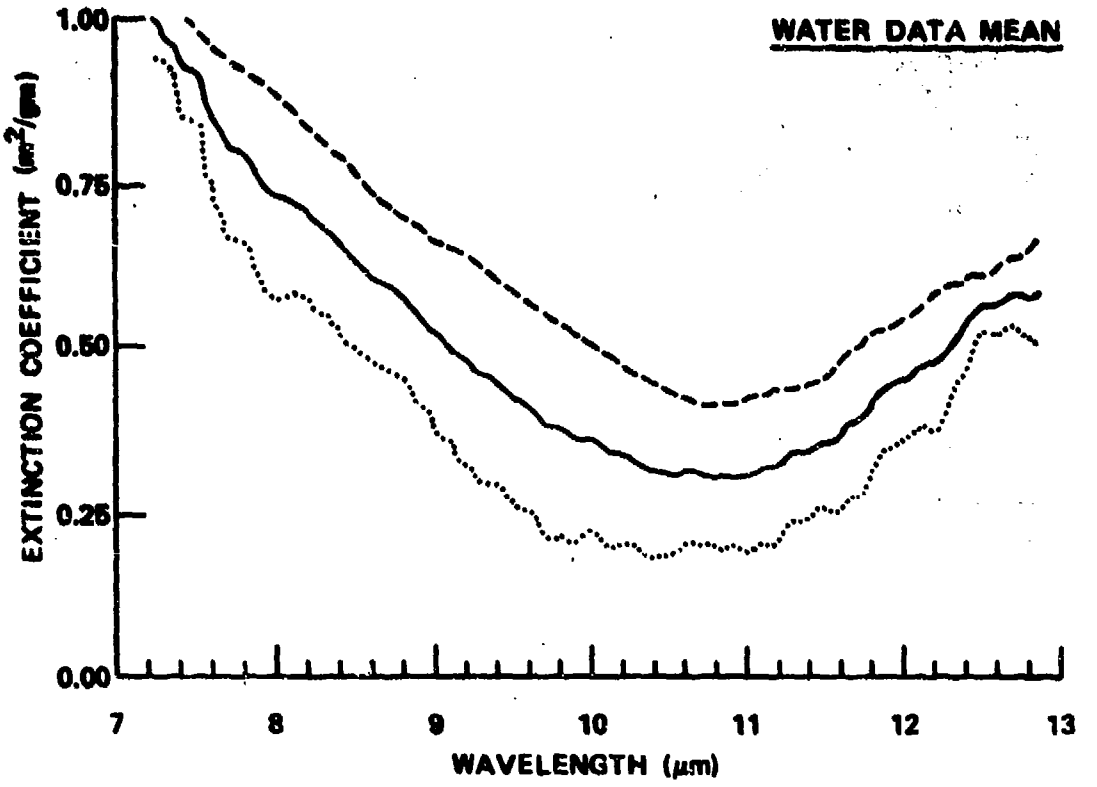

Figure 15. Experimental Data, Water Fog, Average of Five Scans, Estimated 8-μm MMD, 100% RH, Drop Concn = 100% H_2O

Note relative independence of extinction coefficient upon droplet size (i.e., small error for multiple samples) near 12.5-μm wavelength.

In the 3- to 5-μm wavelength region where droplet scattering still predominates but absorption is beginning to be a factor toward longer wavelengths, the resulting extinction is quite flat. In the 7- to 13-μm region (figure 13), a minimum is measured in extinction coefficient near 11.1-μm wavelength where water has a very low real refractive index value (about 1.1). In this region the contributions of droplet scattering and absorption are roughly comparable as components of the total extinction. The tail in figure 13 from 10- to 13-μm wavelength can be compared to those of figures 8 and 11 where water of hydration was a droplet constituent. In limited trials conducted with water fogs on hygroscopic salt nuclei, salts appear to act mainly to dilute the water component in the sense that most salts are spectrally inactive at 7- to 13-μm wavelengths whereas water, a good absorber, now comprises a mass fraction of each drop less than the 1.0 value of fogs or condensed steam. As a result, optical extinctions in this region tend to be lower for fogs of high salt content than for fogs of "pure" water. At the same time, dissolved salts tend to reduce the equilibrium MMD of the resulting aerosol, and this produces more Rayleigh-like scattering behavior at 7- to 13-μm wavelengths so that droplet water absorption then predominates. The subtle interplay between aerosol droplet water content, resulting equilibrium size distribution and spectral extinction are extremely varied, and since ambient humidity and temperature vary temporally, so do resulting optical extinctions of aerosols which have lifetimes comparable to the periods of such variations. At the other extreme, millisecond variations which occur in the droplet condensation and initial growth processes can be studied spectrally with high-speed infrared instrumentation now

becoming available. Because of the complexity of water in the important 7- to 13-μm atmospheric "window" region and the availability of equipment for its study, measurements in this area are being planned.

In figures 14 and 15, averaged infrared spectra are shown for five artificial water fogs under widely differing conditions. While MMD's were near 8 μm and RH was near 100% in each case, other parameters were not sufficiently consistent to be noted on the curves. Rather, figures 14 and 15 are included to show the range of extinction coefficients in randomly-occurring water fogs and that the magnitude of expected extinction, though predictible, may vary by perhaps ±30% or more. Considerable significance is attributed to the rather narrow error distribution near 12.5-μm wavelength (figure 15) where extinction coefficients for the fogs studied showed a consistency of ±10%. In the following discussion, this will be shown to be experimental evidence appearing to substantiate Mie-theory computer predictions that at specific wavelengths in the infrared extinction coefficients would be *nearly independent of droplet size distribution*. This indicates that a simple transmissometer operating, for example, at 12.5 μm should be directly calibratible in liquid water content of its optical path. Thus, a simple solution is suggested to a long-standing problem in meteorological measurements.

V. DISCUSSION OF RESULTS.

Complex refractive index data in the infrared exist in the literature for two of the four aerosol materials which were evaluated, i.e., water[4] and specific dilutions of sulphuric acid.[5] Water can be considered the ultimate dilution case for an acid aerosol. Mie theory calculations had predicted expected scattering, absorption, and total extinction of aerosol clouds for specified droplet size distributions if refractive indices were known. These could be compared directly to experimental data for error analysis. The system water/sulphuric acid suggested itself as the basis for a series of parametric studies leading to an experimentally verified predictive modeling capability for smokes and aerosols of many kinds. Pure water droplets in artificial fogs had MMD's in the 8- to 10-μm-diameter range, while concentrated sulphuric acid nuclei, depending upon the method of their generation, can have sizes ranging toward Aitken diameters of 0.1 μm or less. Between these extremes lies an infinite range of dilutions, each of which will produce equilibrium droplet vapor pressures favoring some droplet size distribution. Furthermore, existing droplets can be modified *in situ*, simply by hydrating them using, for example, steam. Each hydration produces a larger equilibrium droplet size, with attendant changes in spectral extinction characteristics. The system is nearly ideal to produce artificial clouds or smokes for verification studies.

Computer curves such as figure 16, which indicate predicted extinction versus droplet size for 25% by weight sulphuric acid droplets at an illumination wavelength of 10 μm, thus can be used, for example, with figure 11 (for 38% acid drops) to determine agreement between predicted and measured extinctions at a 10 μm wavelength for actual particle MMD's or distributions. In figure 16, the actual MMD of 0.85 μm would lie slightly to the left of the plot, the region where $a_A \approx a_T$.

The flattening of the solid (a_T) curve of figure 16, combined with the merging of this curve with the dashed (a_A - absorption component) curve toward smaller particle sizes, shows that the extinction spectrum at 10-μm wavelength for this smoke which has an MMD near 1 μm should be about 99% due to droplet absorption. The extinction of this smoke at 10 μm wavelength therefore approximates the absorption of the liquid droplets comprising it.

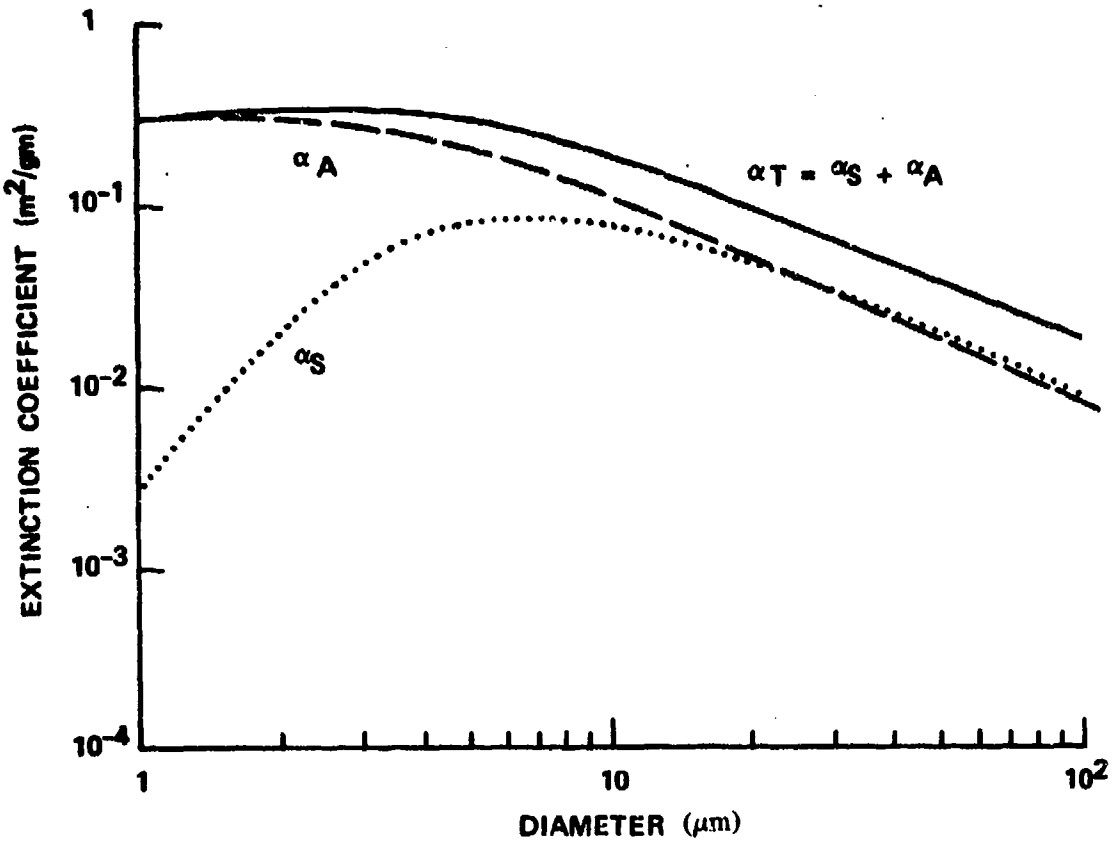

Figure 16. Computed Curves from Data of Palmer and Williams[5] for 25% H_2SO_4 Droplet Aerosol, Showing Total Extinction Coefficient, Absorption, and Scattering Contributions, As Functions of Droplet Diameter, Wavelength = 10 μm

Data comparisons of this type were performed for a wide range of droplet acid concentrations. Figure 11 (for 38% acid droplets) can be compared to figures 17 through 22 which are computer-generated extinction coefficient curves based upon the refractive index data of Palmer and Williams[5] and for a (monodisperse) 1μ droplet diameter. This diameter is close to that obtained experimentally for sulphuric acid smokes, e.g., 0.85 μm. The similarity between figures 11 and 18, both for 38% acid droplets, is particularly interesting. While real aerosols are not monodisperse, the assumption of a constant droplet size in figures 17 to 22 does not introduce significant error if the droplets are small compared to wavelength as they are in this case. Figures 17 to 22 also indicate the extreme nonlinearity of absorption or extinction coefficient at specific wavelengths that would result if this coefficient were plotted against droplet acid concentration. At a wavelength of 10 μm, for example, α_T is 0.16 m^2/gm both at 25% and at 84.5% acid concentration. These effects, due to varying hydrogen bonding in the aerosol droplet solutions, dictate that each dilution of the acid must be treated as a unique material for purposes of measurement of complex refractive index in this wavelength region.

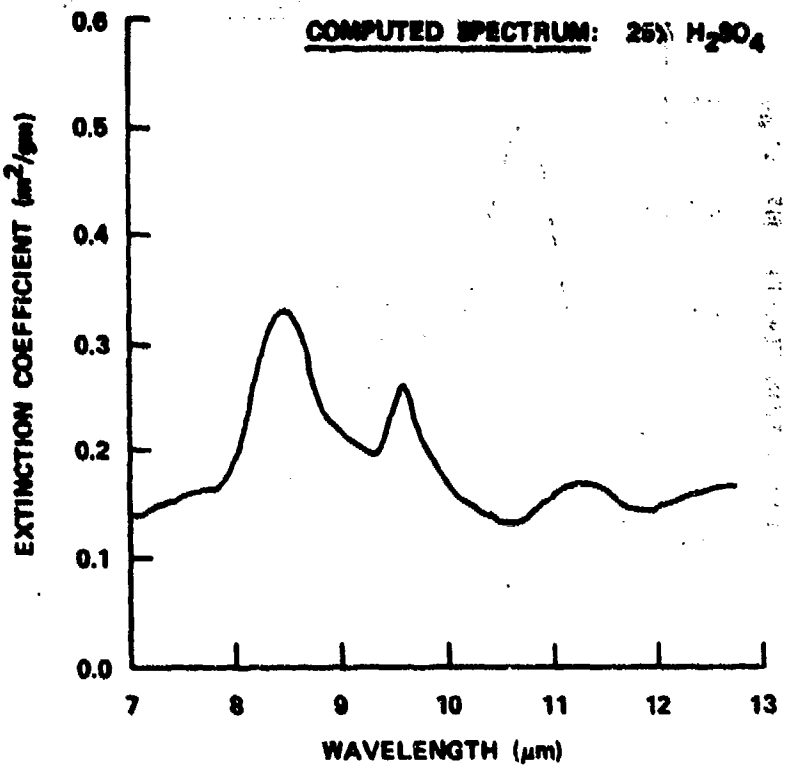

Figure 17. Computed Extinction Coefficient Spectrum from Data of Palmer and Williams[5] for 25% Sulphuric Acid Droplets, 1 Micron Diameter

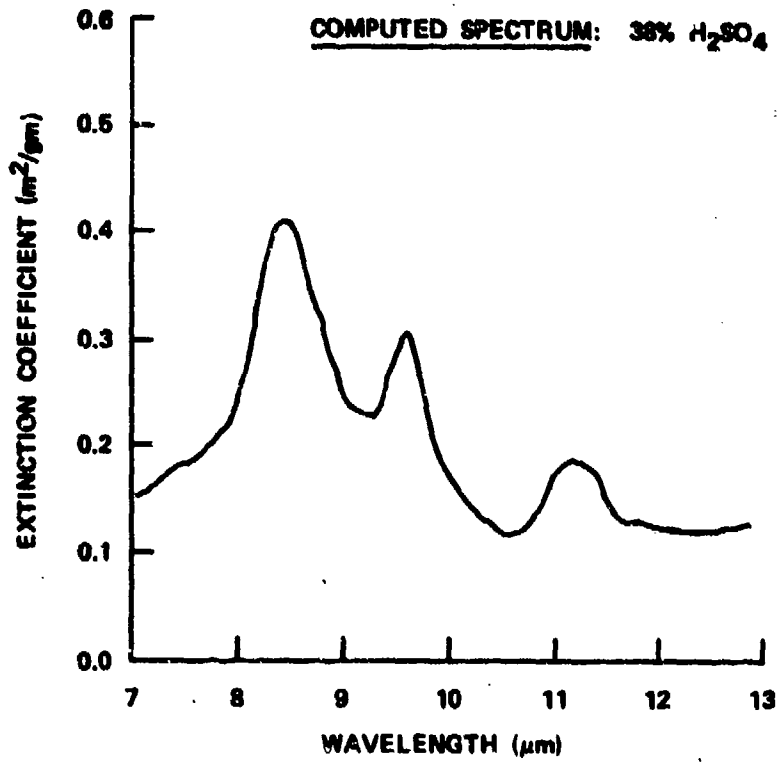

Figure 18. Computed Extinction Coefficient Spectrum from Data of Palmer and Williams[5] for 38% Sulphuric Acid Droplets, 1 Micron Diameter

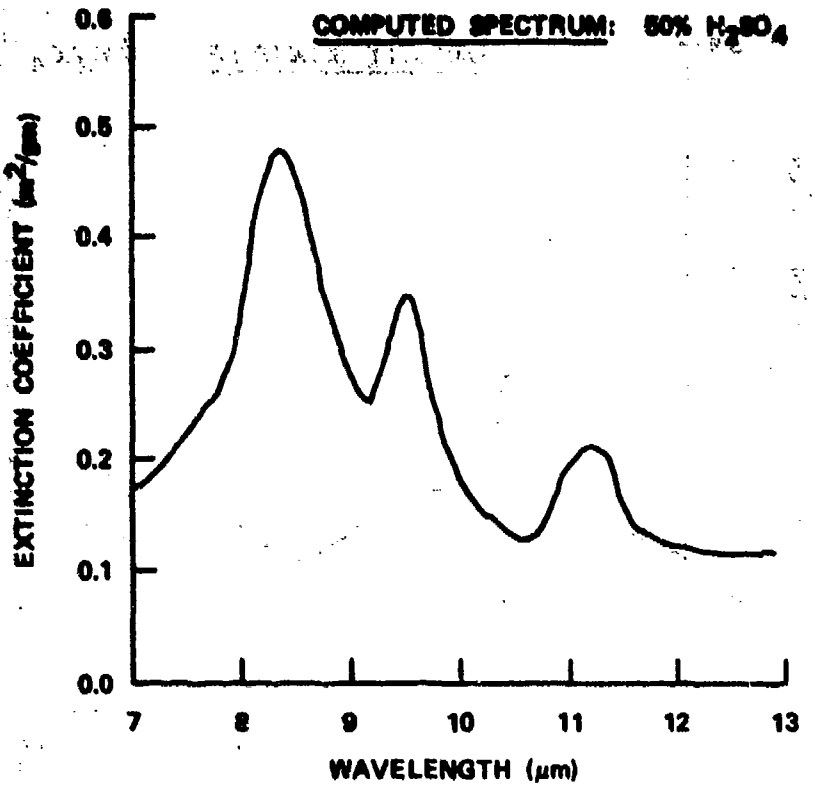

Figure 19. Computed Extinction Coefficient Spectrum from Data of Palmer and Williams[5] for 50% H_2SO_4 Droplets, 1 Micron Diameter

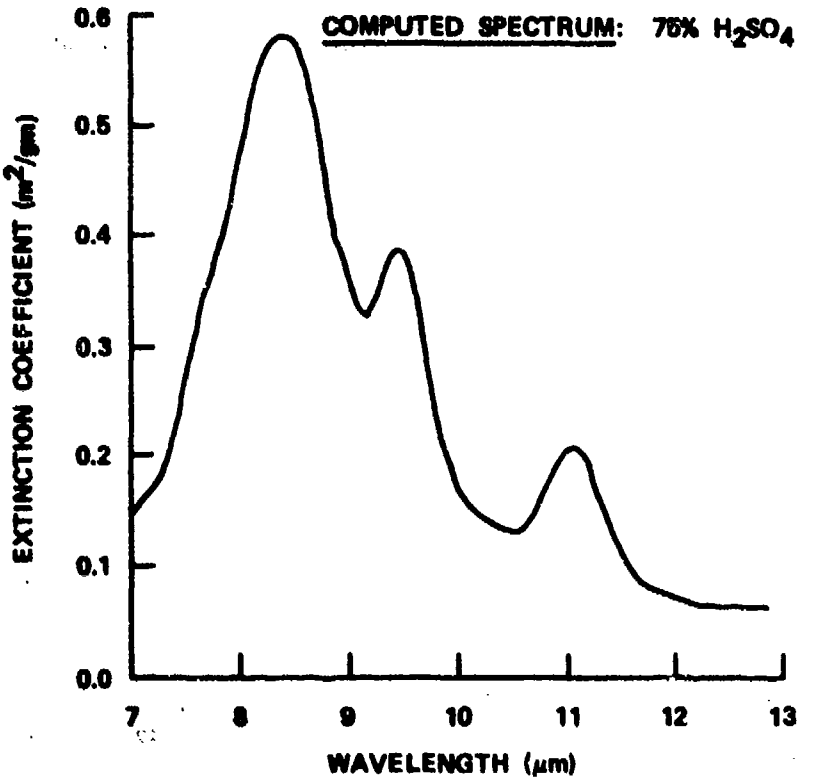

Figure 20. Computed Extinction Coefficient Spectrum from Data of Palmer and Williams[5] for 75% Sulphuric Acid Droplets, 1 Micron Diameter

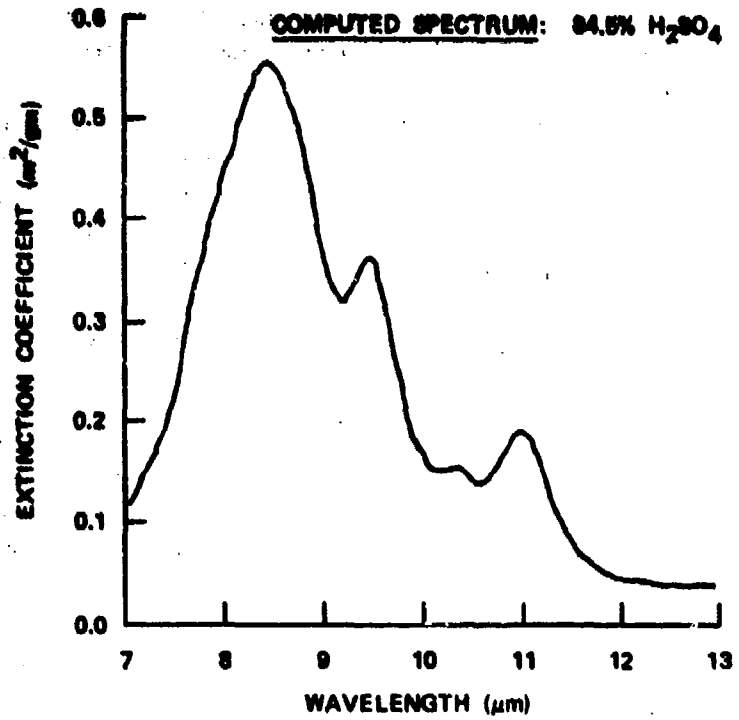

Figure 21. Computed Extinction Coefficient Spectrum from Data of Palmer and Williams[5] for 84.5% Sulphuric Acid Droplets, 1 Micron Diameter

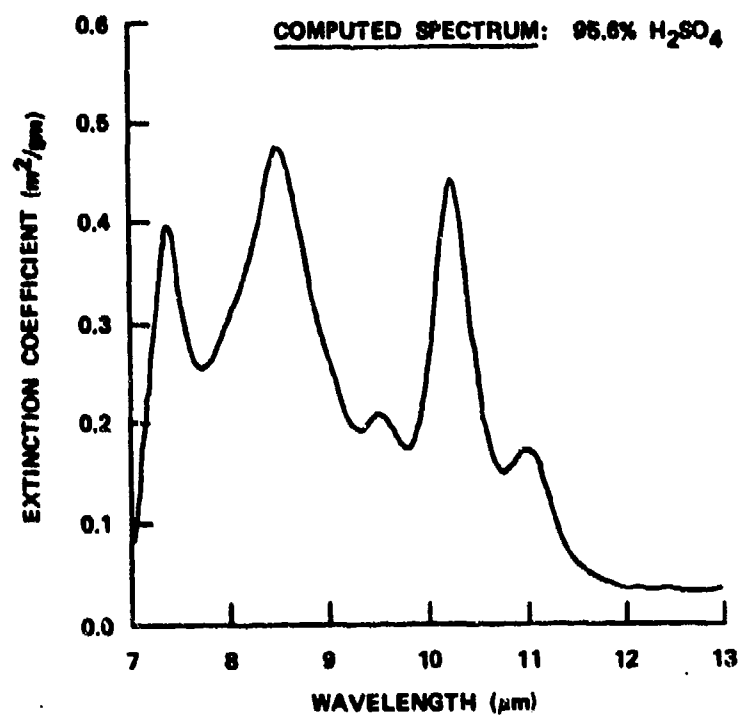

Figure 22. Computed Extinction Coefficient Spectrum from Data of Palmer and Williams[5] for 95.6% Sulphuric Acid Droplets, 1 Micron Diameter

With such parametric complexity, it is not surprising that the spectral behavior of liquid aerosols in the infrared is only recently becoming understood. Yet, comparisons of good experimental data to computed extinction coefficients derived from precise refractive index data have consistently given good agreement. The error between measured and calculated values for the system water/sulphuric acid is about ±20%, and in selected cases as good as ±10%, over wide spectral regions such as the 7- to 13-μm "window." Therefore, predictive modeling at least of acid droplet aerosols should be possible with precision, given that good refractive index data are available. Figures 23 through 25 depict the results of comparative studies of computed versus experimental values of extinction coefficient for an aerosol having a CL (product of droplet concentration, C, gm/m^3, and path length, L, m) of 7.77 gm/m^2 and a droplet acid concentration averaging 38%. By subtracting computed from experimental extinction coefficients for various droplet concentrations, "differential" extinction coefficient plots are obtained such as those in figure 23 through 25. The curves show that best agreement is obtained between computed and experimental data for the case shown by figure 24 where experimental and programmed acid droplet concentrations were very nearly the same. In this case, the experimental results agreed with computed values (using the refractive index data of Palmer and Williams[5]) to within ±15%.

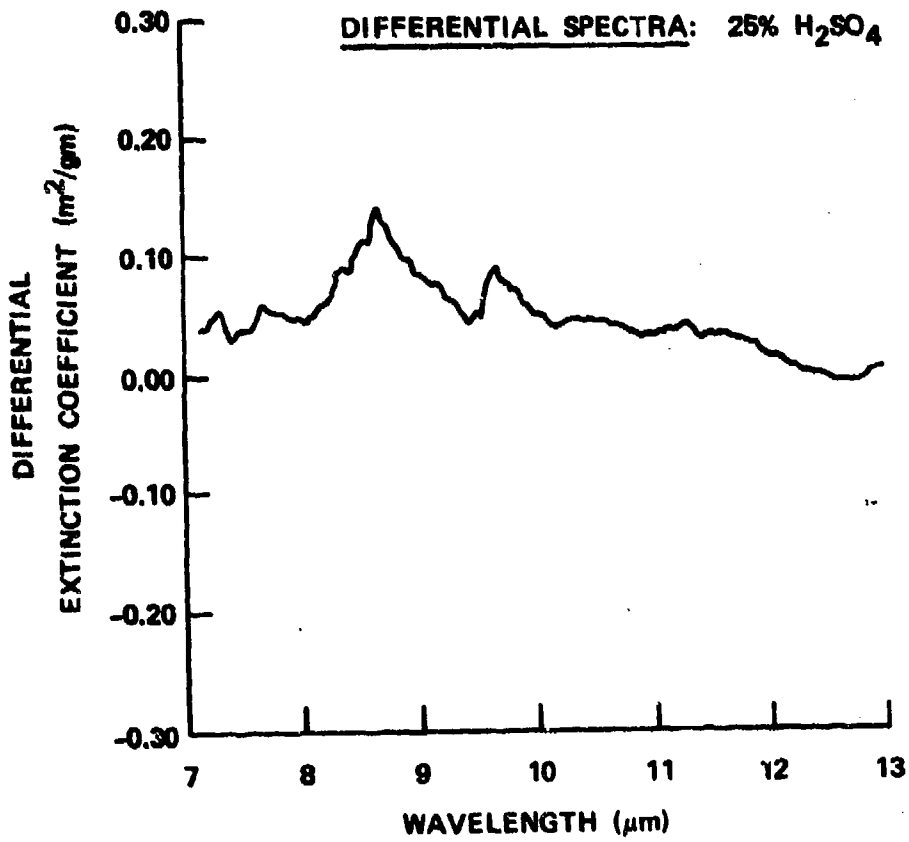

Figure 23. Differential Extinction Coefficients for 25% Sulphuric Acid Droplet Aerosols, Obtained by Subtracting Computed from Experimental Spectra for a Real Aerosol CL = 7.77 gm/m^2

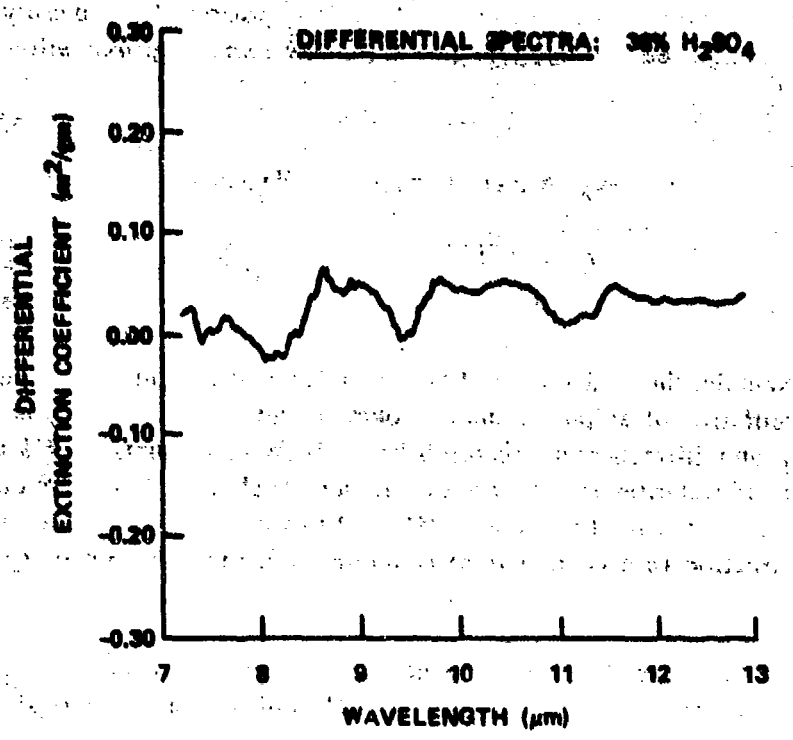

Figure 24. Differential Extinction Coefficients for 38% Sulphuric Acid Droplet Aerosols, Obtained by Subtracting Computed from Experimental Spectra for Real Aerosol CL = 7.77 gm/m^2

Note best agreement (smallest error) for figure 24 compared to figures 23 and 25.

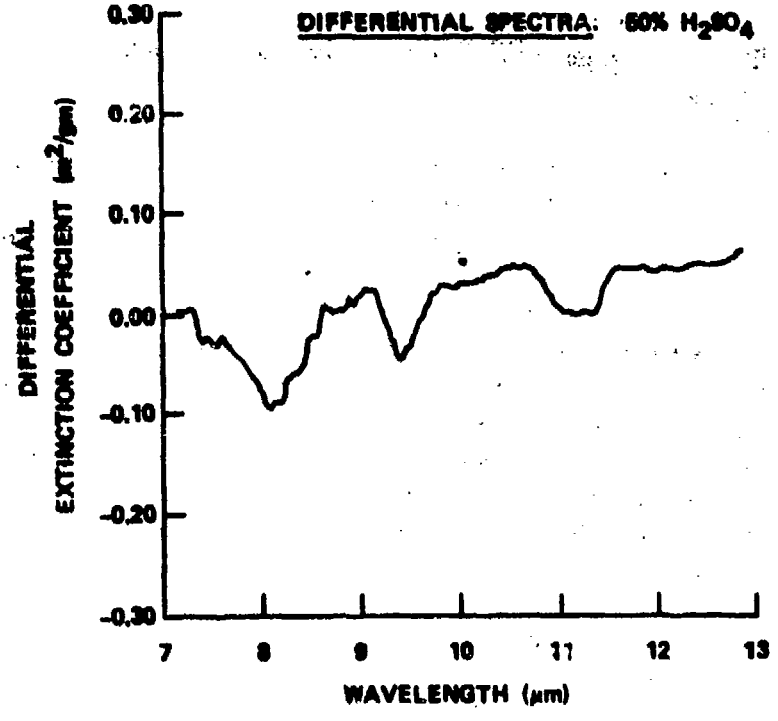

Figure 25. Differential Extinction Coefficients for 50% Sulphuric Acid Droplet Aerosols, Obtained by Subtracting Computed from Experimental Spectra for Real Aerosol CL = 7.77 gm/m^2

Results obtained with sulphuric acid smokes indicate clearly that in Rayleigh-type aerosol scattering situations where droplet absorption predominates heavily over refractive scattering in determining overall extinction, two extremely useful approximation equations can be applied:

$$k_\lambda \cong a_A \rho \approx a_T \rho \qquad (D_\mu << \lambda) \qquad (2)$$

$$\tau \cong (CL)/\rho \qquad (D_\mu << \lambda) \qquad (3)$$

For example, the acid smoke of figure 11 is behaving almost as a pure absorber since figure 16 is representative of sulphuric acid smokes in the 7- to 13-μm region (specifically, the 10-μm wavelength), and differences in spectral behavior between droplets of 25% acid and 38% acid are not large. Figure 16 indicates an extinction coefficient of about 0.25 m^2/gm due almost entirely to absorption (dashed curve) for the 0.85-μm MMD of this smoke. At the same time, the scattering contribution to extinction (dotted a_s curve) is about 0.0025 m^2/gm. Since $D_\mu << \lambda$, equations 2 and 3 will apply.

Equation 2 states that for such smokes the absorption coefficient of a liquid film of the aerosol droplet material, expressed in units $(\mu m)^{-1}$, will be nearly identical to the absorption component of aerosol extinction coefficient a_A (m^2/gm) times the density (gm/cc) of the liquid comprising the droplets, and will approximate the product of total extinction coefficient (m^2/gm), times the density. The units chosen produce the correct numerical value directly. Since the imaginary index of the droplet liquid is related to k_λ by the term $4\pi/\lambda$, aerosol measurements can be used directly to obtain imaginary refractive indices of the droplet liquid. This technique allows refractive index approximations to be made in the absence of directly-measured values. Conversely, we have used thin-film measurements successfully, in work with phosphoric acid, to predict behavior of smokes of this material.

Equation 3 states that where Rayleigh-type conditions exist, the spectral equivalent of a droplet cloud is a liquid film of thickness τ (μm), numerically equal to the CL of the cloud (gm/m^2) divided by droplet liquid density (gm/cc). Thus the smoke cloud of figure 11 could have been simulated spectrally by a liquid film of 38% H_2SO_4, 2.3 μm in thickness since the CL was 3.0 gm/m^2 and the acid density was 1.29 gm/cc. In cataloging transmittance spectra, such equivalent film thicknesses can be used to label families of curves in a meaningful and useful way. For example, the smoke of figure 11 or its equivalent 2.3 μm liquid film would have a transmittance of about 0.47- at 10-μm wavelength. In a spectrophotometer cell, the spectral features of an aerosol cloud can be duplicated by scanning its equivalent liquid film thickness corrected for cell window effects. Spectrophotometer cells have been constructed in the laboratory having window spacings of only a few micrometers (μm), with success. The procedure is less demanding for materials which are optically transparent compared to acid solutions.

Agreement between theory and experiment was obtained of the same precision for water fogs as for acid smokes. The refractive indices of Hale *et al.*[4] allow computation of curves such as figure 26. Since both are for the 10-μm wavelength, figure 26 can be compared directly to figure 16. Because of their small (typically 0.85 μm) MMD's, sulphuric acid smokes in the far

infrared are nearly Rayleigh scatterers, but water fogs with their typical 8- to 10-μm MMD's are Mie scatterers, and equations 2 and 3 cannot be usefully applied to them. However, this complication suggests some interesting techniques for water droplet size determination and for the measurement of aerosol liquid water content in the two examples which follow.

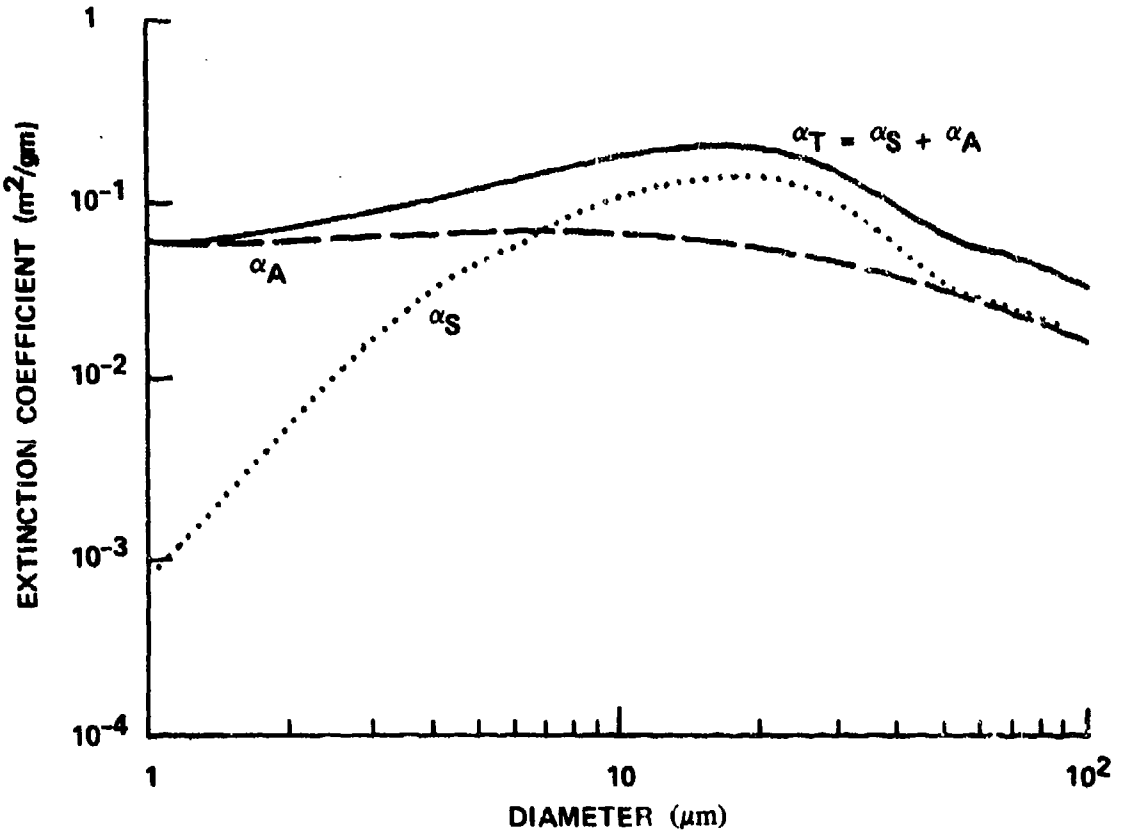

Figure 26. Computed Curves from Data of Hale *et al.*[4] for Water Fog, Showing Total Extinction Coefficient, Absorption, and Scattering Contributions, As Functions of Droplet Diameter, Wavelength = 10 μm

Figure 27 relates optical transmittance of water aerosols at the He:Ne wavelength of 0.63 μm (where nearly all extinction is due to scattering) to transmittance at a composite of wavelengths representing the 8.5 to 12.57 μm spectral region (where real index scattering and droplet absorption contribute about equally to total extinction). The curves are calculated from the indices of Hale and Querry[4] for monodisperse fogs of droplet diameters, D_μ, as labeled on the curves. The points represent experimental data for condensed, cooling steam at 30° to 35°C for a wide range of CL values. They cluster along the curve for $D_\mu = 8$ μm, approximating mean diameters deduced from other measurements. From such observations, generally useful equations and techniques have evolved and some have been reported in reference 2.

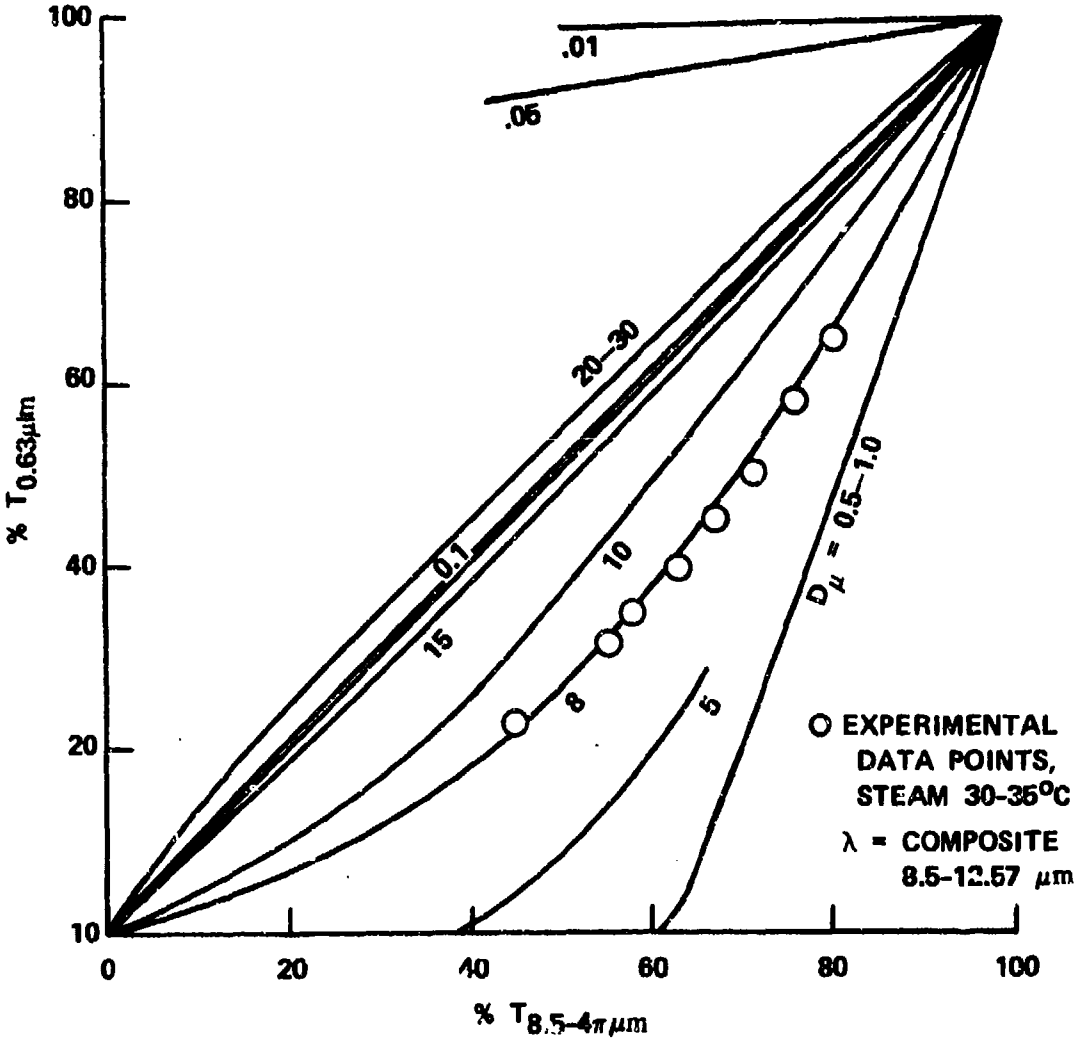

Figure 27. Computed Curves Relating Visible to Far Infrared Optical Transmittance of Water Fog, Showing Experimental Data Points for Condensed, Cooling Steam Clouds

Note that data points cluster along the curve $D_\mu = 8$ μm, in good agreement with gravimetric data from the same experiment.

Figure 28 shows a series of total extinction coefficient curves calculated for various droplet diameters using the refractive indices for water of Hale and Querry.[4] It was noted that because of the manner in which the contributions of refractive and absortive (real and imaginary index) extinction components of water drops combined, as functions of droplet size and wavelength, that total optical extinction coefficients occurred at certain wavelengths which were virtually independent of droplet size.

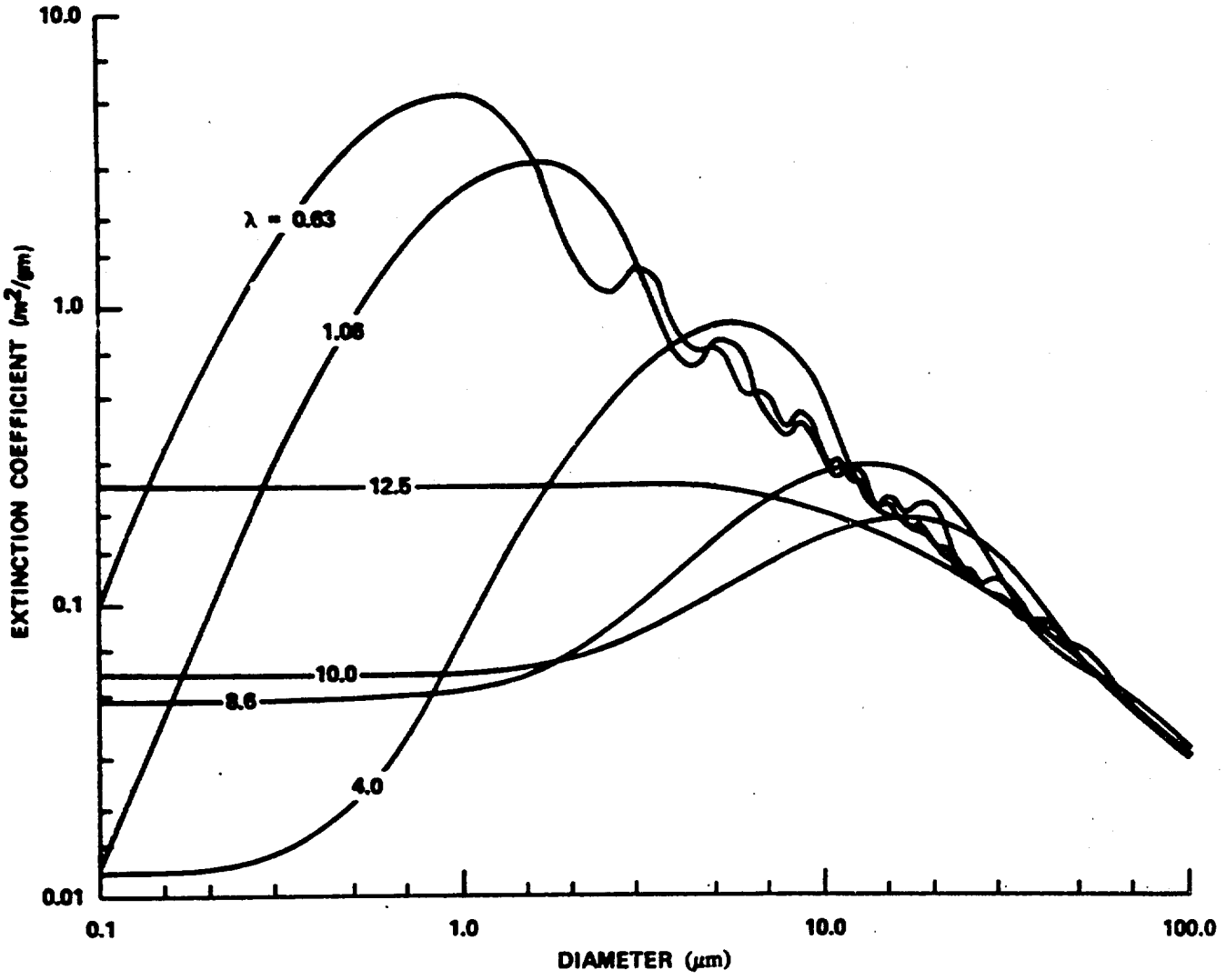

Figure 28. Computed Curves from the Data of Hale *et al.*[4] for Water Fog Relating Total Optical Extinction to Droplet Diameter for a Variety of Visible and Infrared Wavelengths

Note independence of extinction upon droplet size at 12.5-μm wavelength (see figure 15).

Many wavelengths were computed, some of which are included in figure 28, seeking those which would give the flattest possible characteristic. Such a wavelength was found at 12.5 μm, which is fortuitously in a widely-used infrared atmospheric window region. Experimental data for a wide variety of water fogs seemed to confirm the relative insensitivity of the extinction at this wavelength to changing droplet size distributions (see figure 15). Results indicated that a simple transmissometer operating at 12.5 μm was, in fact, an atmospheric total liquid water monitor which could be calibrated directly in mass concentration (e.g., gm/m^3) of liquid water content. Owing to droplet size insensitivity, such a device should integrate water droplets of all sizes, possibly as small as molecular clusters and up to 15-μm diameter (or larger, with decreased precision), into a single water content result. Two patent disclosures were filed covering the technique and an apparatus for this purpose.[6,7] The total extinction coefficient for liquid water content can be read from figure 28 as approximately 0.25 m^2/gm. The technique suggests a simple solution to the meteorologist's long-standing problem of measuring total liquid water content under a variety of circumstances such as observing developing ground fogs or in making cloud measurements from airborne platforms. An accompanying realization was that a wide variety of active and passive infrared instruments already operating at the 12.5-μm wavelength might be effectively monitoring total liquid water content, plus water vapor and other atmospheric constituents, in their optical paths.

LITERATURE CITED

1. Carlon, H. R. Appl. Opt. *10*, 2297 (1971).

2. Manufactured by Anderson 2000, Inc., P. O. Box 20769, Atlanta, GA 30320.

3. Carlon, H. R., Milham, M. E., and Frickel, R. H. Appl. Opt. *15*, 2454 (1976).

4. Hale, G. M., and Querry, M. R. Appl. Opt. *12*, 555 (1973).

5. Palmer, K. F., and Williams, D. Appl. Opt. *14*, 208 (1975).

6. Carlon, H. R. and Frickel, R. H. US Army Edgewood Arsenal Invention Disclosure EA-6594, "Single-Wavelength Monitor for Liquid-Water Content of Clouds and Fogs", Aberdeen Proving Ground, MD 21010, March 1976.

7. Carlon, H. R. US Army Edgewood Arsenal Invention Disclosure EA-6595, "Technique for Liquid Content Measurement of Clouds, Fogs and Smokes". Aberdeen Proving Ground, MD 21010, March 1976.

GLOSSARY

Terms and symbols used in the figures and equations of this paper are as follows:

a_λ	Mass extinction coefficient due to absorption at wavelength λ, m^2/gm $a_\lambda = (1/CL) \ln (1/T_\lambda)$
a_T	Mass extinction coefficient, m^2/gm, consisting of the absorption component of extinction (a_A) which arises from the imaginary index of refraction, plus the scattering component of extinction (a_S)
C	Aerosol droplet concentration, gm/m^3
Drop Concn.	Concentration of major constituent in average droplet, mass percent
D_μ	Droplet diameter, μm
$(I/I_o)_\lambda$	Ratio of transmitted energy at illumination wavelength λ, with aerosol sample in the optical path to that transmitted prior to sample introduction; i.e., aerosol cloud transmittance at that wavelength, unitless
k_λ	Absorption coefficient of the liquid comprising and aerosol droplet at wavelength λ, $(\mu m)^{-1}$
L	Optical path length, m
λ	Illumination wavelength, μm
MMD	Mass median diameter of aerosol droplet size distribution, μm
RH	Relative humidity, percent
σ, σ_g	Geometric standard deviation of aerosol droplet size or extinction coefficient distribution, unitless
T	Optical transmittance through an aerosol cloud, unitless
τ	Precipitable water content of *liquid* in optical path, expressed as an equivalent liquid film thickness, prec. μm
ρ	Density of droplets comprising aerosol cloud (each droplet) gm/cm^3